scientific reports

Check for updates

OPEN

Design and performance evaluation of a spiral bar precision weeding mechanism for corn fields

Wenze Hu[1,2], Syed Ijaz Ul Haq[2], Yubin Lan[2], Zhihuan Zhao[1], Shadab Ahmad[3,4], Areej Al Bahir[5], Junke Zhu[2]✉ & Atiku Bran[6]✉

This paper focuses on addressing the limitations of existing mechanical weeding methods for corn plants by introducing a spiral tendon-type precision weeding device specifically designed for corn fields. The study encompasses mechanical design and theoretical analysis to determine the overall structure, component parts, application scenarios, operation modes, and working principles of the device. The force applied to the spiral tendon weeding cutter head, a crucial working component of the device, is analyzed, along with its motion characteristics. This analysis allows for the calculation of the force required for the spiral tendon to penetrate the soil, as well as the determination of its trajectory and speed in the soil. The desired motion pattern of the weeding cutter head is considered in determining the contour shape of the inner cylinder track and its cooperation mode with the roller follower. Furthermore, the design and optimization of the circulation groove track are conducted to derive the key parameters of the track. A prototype is then constructed based on the proposed structural design and parameter optimization scheme. Soil bin tests are performed to evaluate the device's performance. The optimal combinations of working parameters are determined as follows: a 70-mm depth of the weeding cutter head into the soil, a movement speed of 80 mm/s, and an output thrust of the electric actuator of 180 N. Under these conditions, the device achieves a weed removal rate exceeding 95% with a 3% wounding rate, demonstrating stable operational performance.

Keywords Force analysis, Mechanism design, Motion analysis, Precision weeding, Spiral-bar

Maize (*Zea mays L.*) is a globally significant food crop that plays a vital role in ensuring national economic stability, sustainability and food security[1]. It possesses superior yield potential, resilience, and environmental adaptability compared to other cereal crops[2,3]. However, the presence of weed in maize fields directly reduces yield and quality[4,5]. Consequently, it is crucial to study effective weed control methods in maize fields[6–8].

A variety of approaches have been employed to address weed infestation in fields, including manual weeding, chemical weeding, and mechanical weeding[9,10]. Manual weeding is a labor-intensive process with limited operational efficiency, making it unsuitable for modern agricultural production[3,11]. Chemical weeding can save time and cost but leads to enhanced weed resistance, accelerated community succession, and environmental issues such as air and water pollution[12,13]. Mechanical weeding offers increased efficiency and labor savings compared to manual weeding, as well as eliminates the need for pesticide application[14–16]. Currently, the commonly utilized mid-plow weeder effectively removes weeds in crop rows using specific working parts, such as weeder shovels. However, it faces challenges in removing inter-plant weeds within the crop rows[17,18]. To pave the way for automated precision weeding, the issue of inter-plant weeding must be adequately addressed[19–22].

Weed control devices designed for targeting in-row weeds include toothed rakes[23], hoe-shovels[24], brushes[25], spraying, flaming[26,27], laser-type equipment, and others. Research on intelligent inter-plant weeding devices was initiated in foreign countries during the 1980s[28–30]. However, the current level of intelligence in inter-plant weeding devices remains limited[31]. A system designed for intra-row weeding in field crops, which employs active rotary tines for intra-row weeding and passive tines for inter-row weeding, was introduced in a study

[1]College of Mechanical and Electronic Engineering, Shandong Agriculture and Engineering University, Jinan 250100, Shandong, China. [2]School of Agricultural Engineering and Food Science, Shandong University of Technology, Zibo 255000, Shandong, China. [3]School of Mechanical Engineering, Shandong University of Technology, Zibo 255000, Shandong, China. [4]Centre for Research Impact & Outcome, Chitkara University Institute of Engineering and Technology, Chitkara University, Rajpura 140401, Punjab, India. [5]Chemistry Department, Sirat Obaida Applied College, King Khalid University, Abha 64734, Saudi Arabia. [6]United Nations Development Program (UNDP), Kampala, Uganda. ✉email: zhujunke@sdut.edu.cn; bran.atiku@undp.org

by Chandel et al.[21], introduces a system designed for intra-row weeding in field crops. This system employs active rotary tines for intra-row weeding and passive tines for inter-row weeding. This system uses active rotary tines for weeding between rows and passive tines for weeding within rows. In a separate study by Ye et al.[32], researchers introduced and tested an innovative weed control device designed specifically for soybean fields. This device features elastic comb teeth that reciprocate, moving open and closed around soybean plants to carry out weeding tasks while protecting the crops. Both pieces of research mark significant strides toward advancing mechanical weeding technology, proposing novel solutions to the enduring challenges of weed management in agriculture. Despite these innovations, the studies collectively reveal inherent limitations within the current landscape of inter-plant weeding devices. Notably, these limitations revolve around the precision of the weeding operation and the safeguarding of crops; critical factors that remain to be fully addressed to enhance the efficacy and reliability of mechanical weeding methods. Most related research is still in the theoretical stage of weed identification, with a scarcity of intelligent weeding products used in practical field operations, such as Weed Seeker, Weed-IT, and other weed sensors[33,34]. In China, relevant research on inter-plant weeding has also been conducted. Researchers from South China Agricultural University, including Hu et al.[35], developed a mechanical weeding device for inter-plant weeding in paddy fields based on the residual pendulum motion of weeding claw teeth. Their experiments revealed that increasing the device's forward speed resulted in higher seedling injury rates. Researchers from Northeast Agricultural University designed a cam-rocker-type pendulum weeding device for corn[36] and developed a comb-type weeding device for mid-plowing corn fields using intermittent rotary motion. However, these devices have shown issues with seedling damage, suggesting that research on precision inter-plant weeding equipment in China, especially in the realm of intelligent weeding technology, is still in its early stages.

This paper resolves specific issues and explains how the spiral-bar weeding can solve the issues by proposing the design of a spiral bar-based precision weeding device. Contemporary methodologies for inter-plant weed management in maize cultivation predominantly employ a seedling-avoidance strategy, distinguished by its imprecision and elevated propensity for crop detriment. Despite its prevalent adoption, this strategy frequently fails in the meticulous eradication of weeds, highlighting the critical deficiencies inherent in such approaches—primarily their lack of precision. These limitations vividly accentuate the pressing necessity for innovative interventions capable of meticulously balancing efficacious weed extermination with the preservation of crop integrity. In response to these challenges, our study introduces a novel approach that diverges significantly from conventional practices. Instead of the broad and indiscriminate strategy of seedling avoidance, our research focuses on directly addressing each weed individually. By implementing a method that targets weeds on a per-plant basis, we aim to significantly enhance the precision of weed control operations within cornfields. This tailored approach not only promises to improve accuracy in removing unwanted plants but also substantially reduces the likelihood of causing harm to the corn seedlings themselves. Leveraging exhaustive mechanical design, theoretical scrutiny, and empirical corroboration, authors are introducing a spiral tendon-type precision weeding apparatus, expressly engineered for maize fields. The term 'spiral tendon' in this context refers to a spiral-shaped weeding component designed to engage with the soil in a helical motion, allowing for precise weed removal, reducing soil disturbance and minimizing damage to surrounding crops. This design enhances the precision of the weeding process, particularly in inter-plant spaces where conventional tools may struggle to operate without harming crops. This invention endeavors to surmount the challenges prevalent in extant mechanical weeding paradigms by providing an innovative and pragmatic remedy. Concentrating on meticulous soil penetration and tailored motion trajectories for the direct targeting of each weed, our methodology heralds a substantial progression in agricultural engineering and mechanized agronomy. It aims to elevate the weed removal efficacy while concurrently mitigating the risk of collateral damage to maize seedlings.

Materials and methods

Overall structure

In the study, a precision weeding device featuring a spiral bar design was developed. This device comprises several components, including a motorized actuator, an outer cylinder, an inner cylinder, a bearing, a roller follower, a spiral bar weeding cutter head, and a spring-loaded top blade. The structure of the device is illustrated in Fig. 1.

To enhance its functionality, the device is mounted on an intelligent navigation trolley and used in conjunction with a weed identification system. It is primarily applicable for weeding in cornfields during the 3 to 6-leaf stage. During the experiments conducted within this study, weeds are identified and located through a machine vision system. During operation, a camera captures images of the weed which are then processed by a deep learning model to detect and ascertain the positions of weeds. For operational deployment, this deep learning model[37], is executed on an embedded development board mounted on the vehicle designed for field navigation and weed control.

Working principle

During field operation, the weed recognition system detects the precise location of the weeds and promptly transmits a signal to initiate activation of the motorized actuator. The generated force is then efficiently transmitted to the inner cylinder through the actuator, establishing a direct mechanical connection with the weeding cutter head. This synchronized motion propels the weeding cutter head to engage in precise, targeted movement. Following points gives detail about motion and equipment response capacity.

a. During the weeding action, the trolley remains stationary while the weeding device performs its operation. The stationary position allows for precise targeting and removal of weeds as detected by the machine vision system. The weed identification system is seamlessly integrated with the spiral bar weeding device and the

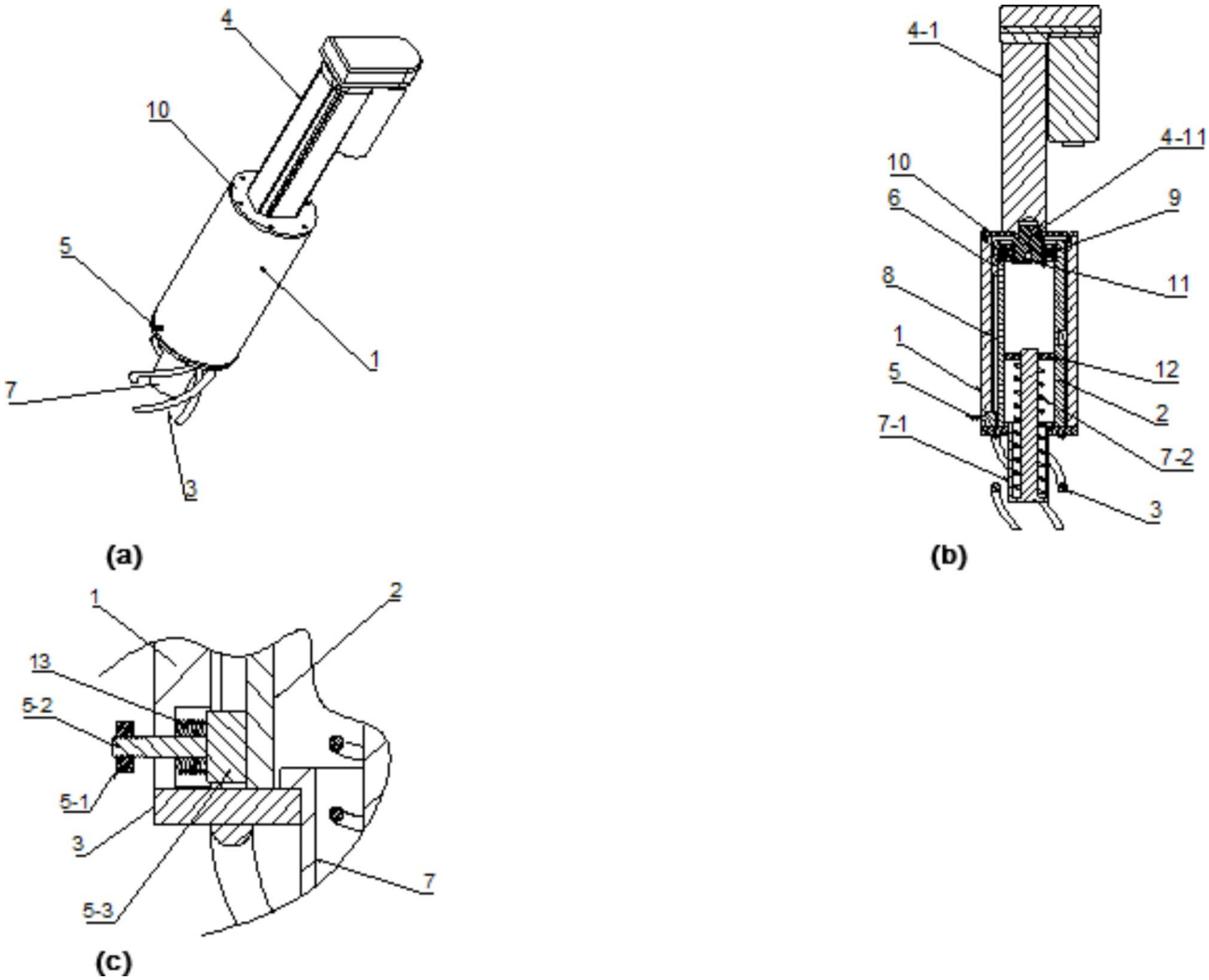

Fig. 1. Structural diagram of the spiral-bar weeding device. (**a**) 3D diagram of spiral-bar weeding device. (**b**) Cross-section view of spiral-bar weeding device. (**c**) Partial diagram of roller follower installation. (1) Outer cylinder (2) Inner cylinder (3) Weeding head (4) Electric drive mechanism 4-1. Electric push rod 4–11. Telescopic rod connector (5) Roller Follower 5-1. Limit nut 5 -2. Installation column 5-3. Sliding column (6) Spiral chute (7) Elastic adaptive shirk component 7-1. Removing parts 7 -2. Adaptive spring (8) Vertical chute (9) Bearings (10) Connection board 11. Limit baffle 12. Partitions 13. Compression spring.

intelligent navigation trolley through a real-time data processing unit. The system uses a camera mounted on the trolley to capture images of the field, which are then processed by a deep learning model running on an embedded platform. Once weeds are detected, the system immediately sends signals to the motorized actuator of the weeding device, ensuring synchronized operation between weed detection and weeding actions. Synchronization challenges, such as delays between detection and actuation, were mitigated by optimizing the processing speed of the detection algorithm and the response time of the motorized actuator.

b. The system is designed to respond to weed detection signals within milliseconds. Specifically, the time delay between weed recognition and the activation of the motorized actuator is approximately 100–150 milliseconds, depending on the complexity of the field conditions and the processing load on the embedded system. This rapid response ensures that the weeding device operates efficiently without significant lag, maintaining high precision in targeting and removing weeds.

It is essential to note that the prime focus of this paper is on the design and testing of the weeding device, while the weed recognition system is utilized solely as a tool to verify the effectiveness of the weeding device. The weed recognition system uses a camera to capture field images, which are processed by a deep learning model to identify the location of weeds. The system then sends a signal to activate the actuator of the weeding device. However, the weed recognition system is not the central subject of this study but rather a supportive component used to validate the precision and effectiveness of the weeding mechanism. Figure 2 shows the architectural diagram of the weed recognition system integrated into the weeding device.

Fig. 2. Architectural diagram of the weed recognition system integrated into the weeding device.

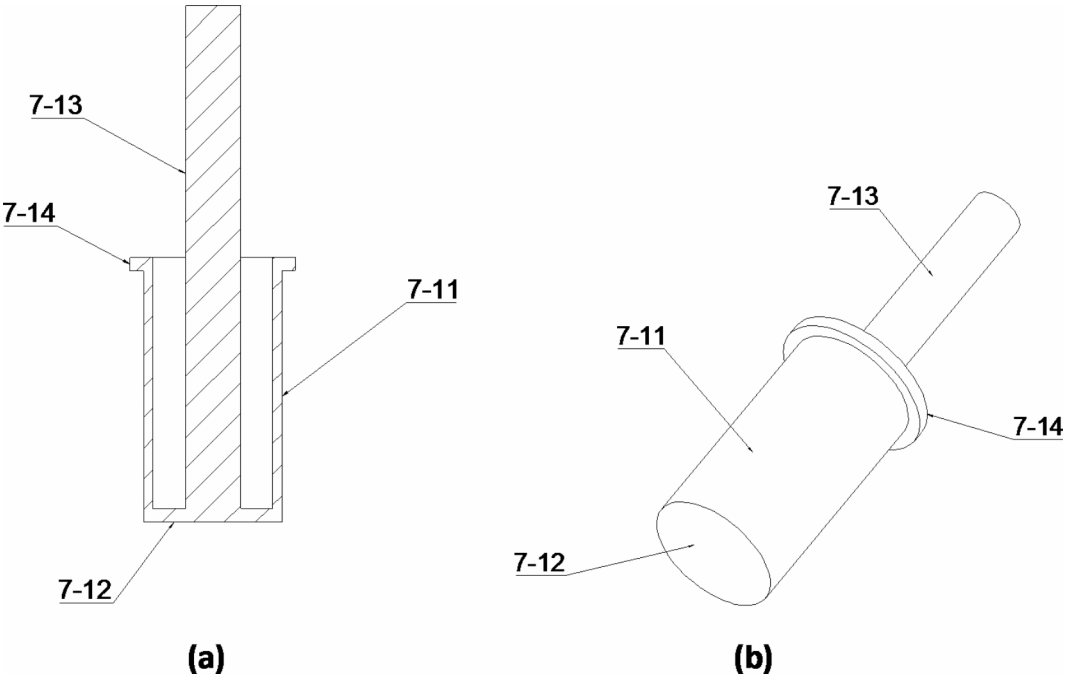

Fig. 3. Structural diagram of push-off parts. (**a**) Sectional view of push-off parts. (**b**) 3D drawing of push-off parts. 7–11. Guide cylinder 7–12. Push plate 7–13. Guide column 7–14. Limiting part.

To facilitate controlled rotation of the inner cylinders within the annular space between the outer and inner cylinders, a precision guiding assembly is employed. This guiding assembly consists of roller followers affixed to the internal surface of the outer cylinder and a cyclic track set on the outer circumference of the inner cylinder. The track exhibits an intricate pattern of spiral grooves and vertical grooves, allowing for the conversion of linear motion into a spiral downward and vertical upward circular motion. This orchestrated motion is subsequently transmitted to the weeding cutter head, enabling it to spiral into the soil, pull out the weeds vertically, and separate them from the surrounding soil. As the weeding cutter head rotates, the weeds are wrapped inside the cutter head.

To remove the weeds from the weeding cutter head, an elastic adaptive push-off assembly is present on both the inner cylinder and the weeding cutter head as illustrated in Fig. 3. This assembly not only automatically removes the weeds but also adaptively slides along the axial direction of the inner cylinder. This adaptability allows the weeder to insert into the soil, pull out the weeds, and then unload them automatically. The operation process is simple, resulting in high weeding efficiency while saving time and labor.

Key components design and analysis

Weeding cutter head

The structure and performance of the spiral bar weeding cutter head play a crucial role in the weeding effect and working efficiency, based on the working requirements of the spiral rib weeding device in this section, it will be discussed the structure scheme of the weeding cutter head by analyzing these requirements.

When designing the weeding parts, it is essential to consider the specific crop being planted, the practical field operation conditions, as well as the desired weeding action. For example:

① Maize planting typically has row spacings ranging from 50 to 60 cm for general planting, 33–40 cm for spring sowing, and 25–33 cm for summer sowing.

The weeding parts need to facilitate inter-plant weeding while ensuring minimal damage to the seedlings. This imposes specific size and operational accuracy requirements on the weeding components.

② To effectively remove common weeds like wheat seedlings, Matang, and dog-tail in cornfields, the weeding parts need to penetrate the soil to a depth of 7–10 cm, as recommended by agronomy. This ensures a high success rate of weeding.

Additionally, the design should fulfill other technical requirements such as simplicity, adaptability, low power consumption, and low vibration.

Considering these requirements, this paper proposes a design for the spiral bar weeding part, which consists of four spiral metals and a connecting base plate, as shown in Fig. 4.

Force analysis of spiral bar

In Fig. 5, the force acting on the tip of the spiral bar during penetration of the weeding device into the soil is depicted. The resistance of the soil to the spiral bar is denoted as F1, while the thrust force exerted by the electric pushrod on the spiral rod is denoted as F2. It is evident that the spiral bar generates extrusion force on the soil, causing soil deformation under this pressure.

Additionally, the thrust exerted by the electric actuator on the spiral bar is also a contributing factor to this extrusion force. At this stage, the soil experiences a uniaxial stress state, characterized solely by positive stress

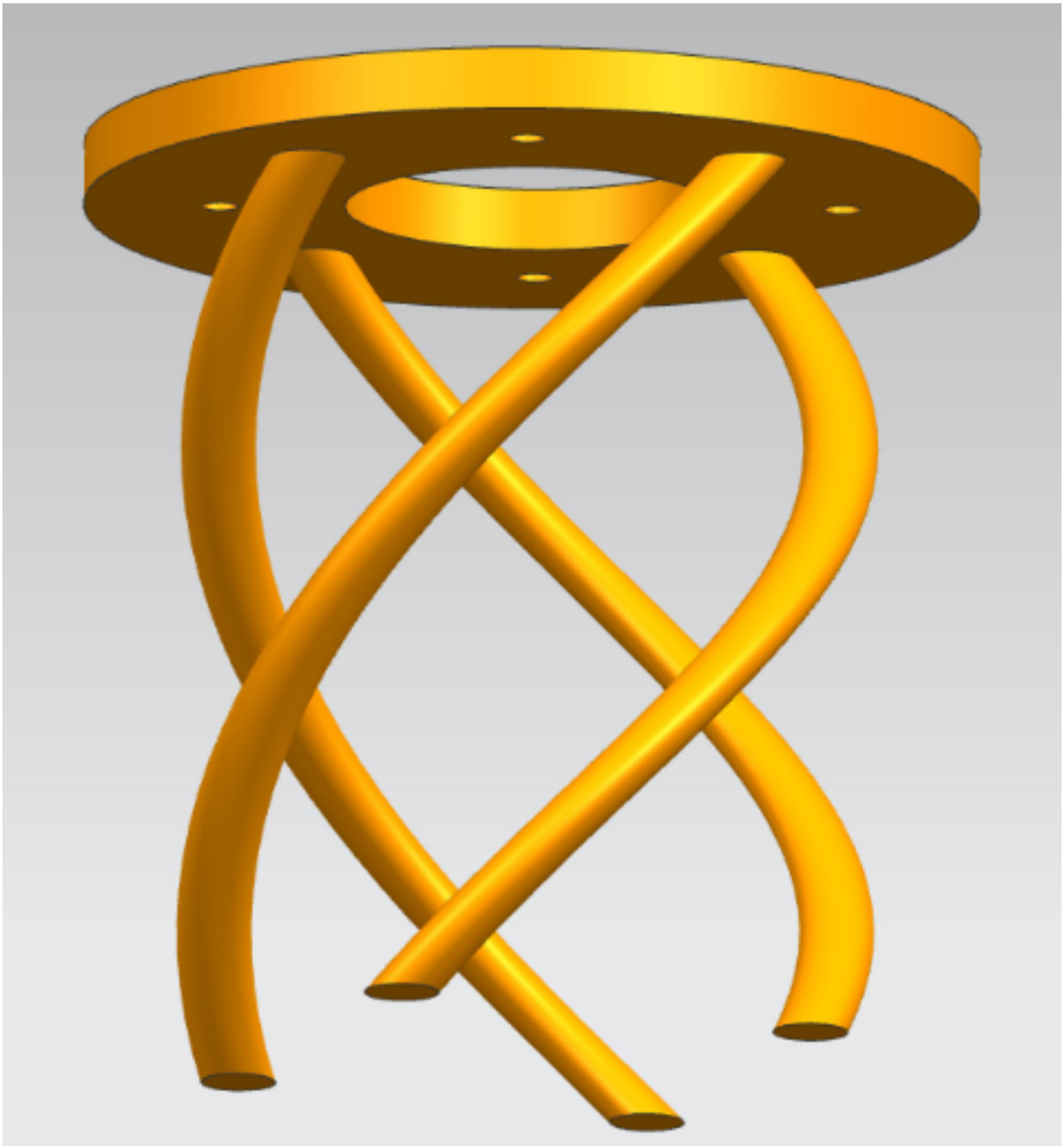

Fig. 4. Spiral-bar type weeding head (CAD design developed using NX 12.0).

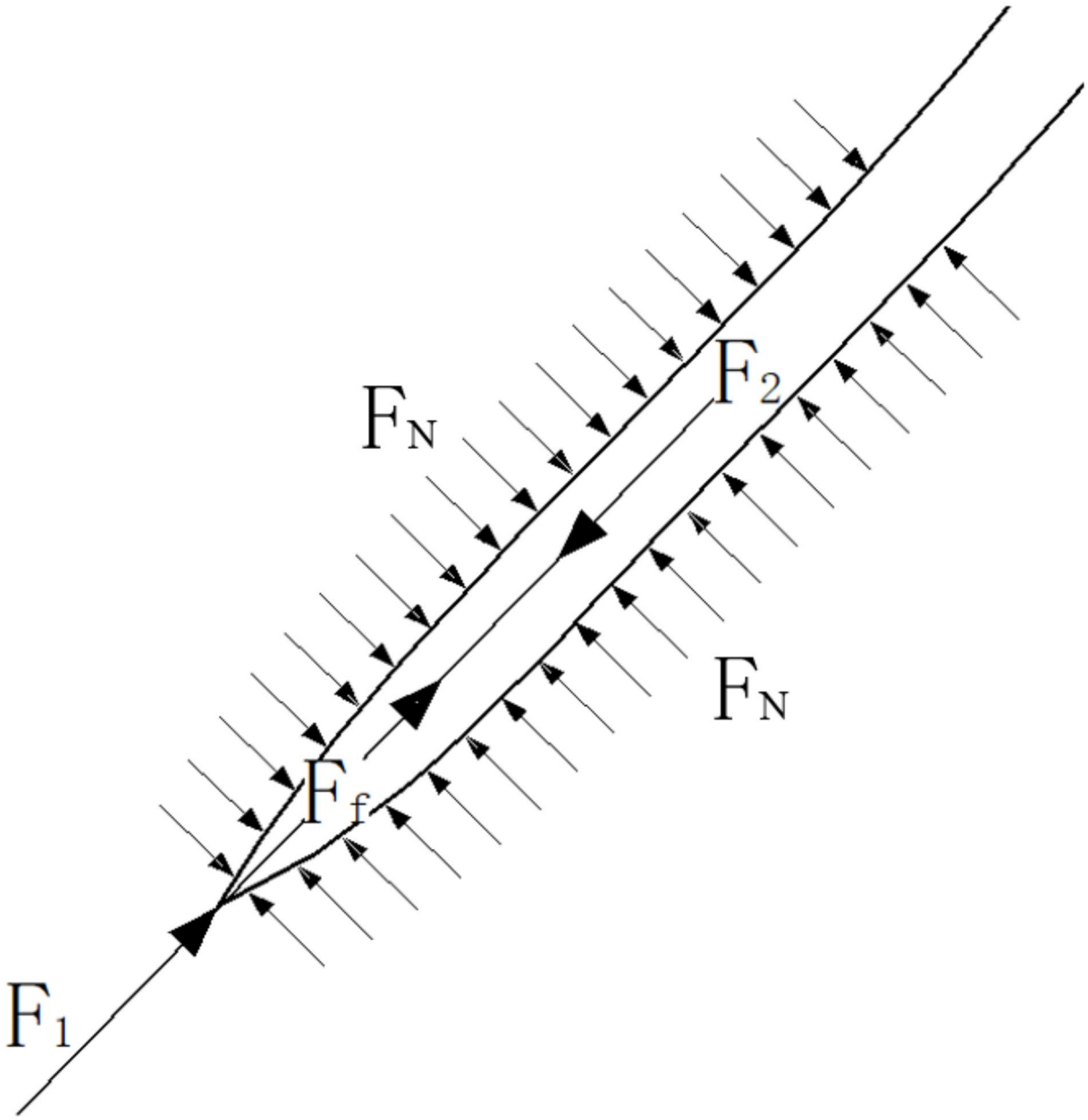

Fig. 5. Force diagram at the tip of the spiral bar. F_1 is the normal resistance of the soil to the tip of the spiral-bar. F_2 is the thrust force exerted by the electric push rod on the spiral-bar. F_f is the sliding friction force of the soil against the spiral-bar. F_N is the positive pressure of the soil on the spiral-bar.

without any shear stress. This positive stress corresponds to the maximum principal stress of soil damage, as described by the Mohr–Coulomb Failure Criterion[38], which is expressed by Eq. (1). Some assumptions made regarding soil properties in the application of the Mohr–Coulomb Failure Criterion;

a. Soil behaves elastically until failure.
b. Cohesion is constant for a specific soil type.
c. Internal Friction Angle (φ) is constant for a given soil type under specific conditions.
d. Straight-line failure envelope in Mohr stress space.
e. Failure occurs at specific points on the failure envelope.
f. Soil is assumed to be homogeneous and isotropic.
g. Instantaneous failure without considering time effects.
h. Primarily two-dimensional stress states assumed.
i. Pore water pressure is not accounted for unless modified.

$$\sigma_1 = 2Ctan\left(45^\circ + \frac{\varphi_1}{2}\right) \tag{1}$$

where: σ_1 is the maximum principal stress of soil damage suggested by Al-Awad[39]; C is the soil cohesion, Pa; φ_1 is the angle of internal soil friction, °.

Therefore, the normal resistance acting on the tip of the spiral bar is given by Eq. (2).

$$F_1 = \sigma_1 S \tag{2}$$

where: F_1 is the normal resistance of the soil to the tip of the spiral bar, N; σ_1 is the maximum principal stress of soil damage, Pa; S is the normal cross-sectional area of the spiral reinforcement, m^2.

The sliding friction of the soil on the rest of the spiral bar satisfies Cullen's formula as shown in Eq. (3).

$$F_f = \mu\left(F_N + F_p tan\varphi_2\right) \tag{3}$$

where: F_f is the sliding friction of the soil on the spiral bar, N; μ is the dynamic friction factor between the soil and the spiral bar; F_N is the positive pressure of the soil on the spiral bar, N; F_p is the adhesion force of the soil on the surface of the spiral bar, N; φ_2 is the friction angle between the soil and the spiral rib, °.

The thrust of the motorized actuator on the spiral bar is the sum of the normal resistance of the soil to the spiral bar and the friction, as in Eq. (4).

$$F_2 = F_1 + F_f \tag{4}$$

This gives the force required for the spiral bar to enter the soil.

Motion analysis of weeding cutter head

The weeding cutter head penetrates the soil while simultaneously combining downward movement with rotational motion along the circumferential direction. This movement is achieved by the linear motion output of the electric actuator synchronized with the guided spiral track, resulting in a spiral trajectory, as depicted in Fig. 6.

The parameters of the helix and the speed of the electric actuator's linear and circumferential rotations are analyzed to determine the movement characteristics of the weeding cutter head.

Considering the growth of weed roots, the initial parameters for the weeding cutter head are as follows: an entry depth is 7 cm, the diameter is 6 cm, and evenly distributed spiral ribs around the 6 cm circumference. The determination of these parameters is based on agronomic research and preliminary testing. The initial parameters were determined based on the average root depth of common weeds and the standard spacing between corn plants. Referring to Fig. 6, the initial position of the spiral bar's tip is denoted as A0. The linear speed of the motorized actuator is v_z, the movement time is t_1, and the corresponding movement distance in the vertical direction is s_1. The vertical coordinate is represented by z_1 and can be calculated as

$$z_1 = s_1 = v_z t_1 \tag{5}$$

Simultaneously, guided by the interaction between the spiral groove and the roller followers, the spiral bar undergoes a rotation angle of ϕ_1, resulting in its actual position, denoted as A1. As the motorized actuator continues to move, additional coordinates in the vertical direction, such as z_1, z_2, z_3, …, and the corresponding positions of the spiral bar, A1, A2, A3…, are obtained. The smooth curve connecting these points represents the actual trajectory of the spiral bar.

Based on the coordinate directions shown in Fig. 6, we can express the parametric equation for the actual trajectory of the spiral bar as (Eq. 6).

$$\begin{cases} x = Rcos\left(\frac{3}{4}\pi - \omega t\right) \\ y = Rsin\left(\frac{3}{4}\pi - \omega t\right) \\ z = v_z t \end{cases} \tag{6}$$

In the formula:R is the radius of rotation of the tip of the spiral bar, m; ω is the rotational angular velocity of the spiral bar, rad/s; v_z is the motorized actuator output speed, m/s; t is the time parameter, s.

Equation (6) is the derivative of 't', then derivation of the actual velocity of motion of the spiral bar in x, y, and z, axes can be obtained as Eq. (7).

$$\begin{cases} v_x = \frac{dx}{dt} = \omega Rsin\left(\frac{3}{4}\pi - \omega t\right) \\ v_y = \frac{dy}{dt} = -\omega Rcos\left(\frac{3}{4}\pi - \omega t\right) \\ v_z = \frac{dz}{dt} = v_z \end{cases} \tag{7}$$

Therefore, the actual velocity of the spiral bar is Eq. (8).

$$v = \sqrt{v_x^2 + v_y^2 + v_z^2} = \sqrt{R^2\omega^2 + + v_z^2} \tag{8}$$

Set the velocity ratio of circular and linear motion to 1, which is calculated as Eq. (9).

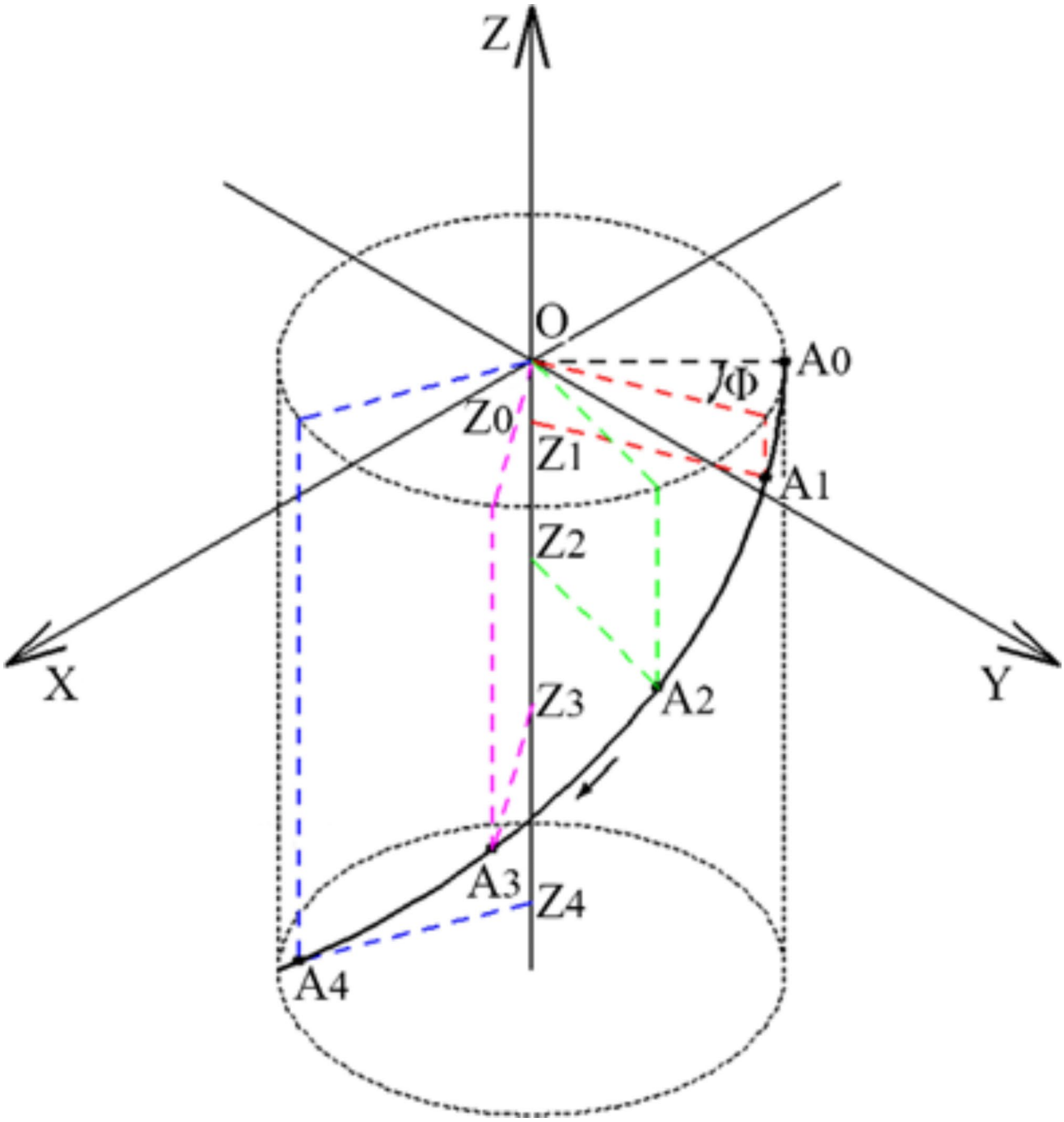

Fig. 6. Trajectory of the spiral bar.

$$\lambda = \frac{\omega R}{v_z} \tag{9}$$

Where, λ is the ratio of velocity in the circumferential direction to the vertical direction.

The angle of rotation 'ϕ' of the spiral bar can be obtained as below Eq. (10);

$$\phi = \omega t = \frac{\lambda v_z}{R} t \tag{10}$$

From this, the trajectory and velocity of the spiral bar in the soil can be obtained.

Inner cylinder and roller follower

The upper end of the inner barrel is connected with the output shaft of the electric actuator through a bearing, while the lower end is fixed with the weeding cutter head through the bolt. The primary role of the inner barrel is to transmit the force and motion from the electric actuator to the weeding cutter head, so it has the same motion law with the weeding cutter head, according to the above analysis of the motion of the weeding cutter head, the motion trajectory of the weeding cutter head into the soil process is a helix. Consequently, the inner barrel is designed to convert the linear motion of the electric actuator into this spiral motion.

The outer wall of the inner cylinder features a circular groove track which was designed to accommodate the roller follower. This track consists of two parts, one is spiral groove and other one is a vertical groove (as illustrated in Fig. 7a). This circular track can be utilized to convert the straight-line motion of the electric actuator into a spiral downward and vertically upward cyclic motion transmitted to the weeding cutter head. The specific shape of the spiral track depends on the motion trajectory of the weeding cutter head. Therefore, a comprehensive analysis of the weeding cutter head's motion is essential for designing an appropriate curve shape for the track. The parameters of the spiral track can be obtained through analysis, as in Eq. (11).

$$s = l/(2) \tag{11}$$

where: s is the axial travel distance; l is the spiral orbital lead, and since the number of spiral thread heads is 1, it is also the pitch; ϕ is the angle of rotation in the circumferential direction, having unit in 'rad'.

The length of the vertical chute equals the pitch of the spiral chute, and the vertical track extends along the axis of the inner cylinder. Its lower end connected to the lower end of the spiral track, and its upper end connected to the upper end of the spiral track, thus forming a closed loop.

The depth of the spiral groove gradually decreases in the upward direction of the spiral, while the depth of the vertical groove gradually decreases in the downward direction of the vertical. Specifically, the depth of the upper end of the spiral groove is smaller than that depth of the upper end of the vertical groove; and the depth of the lower end of the spiral groove is larger than that depth of the lower end of the vertical groove.

In conjunction with the track is a roller follower fixed on the outer cylinder (as shown in Fig. 7b). A compression spring is positioned between the roller follower and the inner wall of the outer cylinder to exert pressure on the roller follower against either the spiral groove or the vertical groove. One end of the compression spring acts on the outer cylinder, while the other end acts on the spiral groove or the vertical groove. Since the depths of the spiral and vertical slots differ, the compression spring is set to ensure that the follower is always pressed against the spiral or vertical slots to ensure that the follower can automatically switch to fit on the spiral or vertical slots.

The initial position of the roller follower is under the action of the compression spring, against the deepest position at the lower end of the spiral groove. When driven by the electric actuator, the inner cylinder moves downward, causing the roller follower to traverse the spiral track. In this joint motion with the inner cylinder,

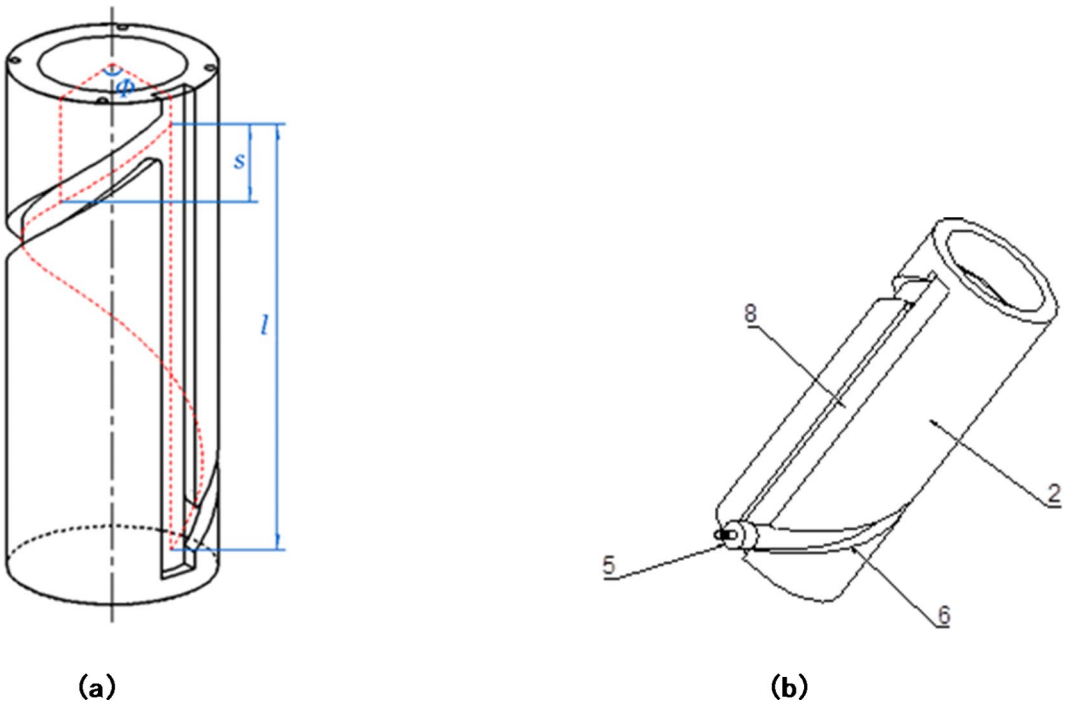

Fig. 7. Schematic diagram of inner and outer cylinders: (**a**) Schematic diagram of inner cylinder track; (**b**) Matching Schematic diagram of inner cylinder and roller follower. 2. Inner cylinder 5. Roller follower 6. Spiral slide 8. Vertical slide.

the roller follower follows a downward spiral path, making it easier for weeding cutter head to penetrate the soil. When the inner cylinder reaches its lowest point, the roller follower transitions from its shallowest position at the upper end of the spiral track to the deepest point at the upper end of the vertical groove due to the spring's force. During the weed-pulling process, the electric actuator drives the inner cylinder upward, causing the roller follower to move within the vertical track, Simultaneously, the inner cylinder goes upward along the vertical direction, and the follower moves from the shallowest position at the upper end of the vertical groove to the shallowest position at the lower end of the vertical groove. It then proceeds to enter the shallowest position at the lower end of the spiral groove, completing the reset process in preparation for the next weed-pulling operation.

Tests

Test conditions

The test bed for the spiral tendon type precision weeding device was constructed in April 2023 at the soil trough laboratory of Shandong University of Science and Technology. The purpose of this test setup is to evaluate the operational performance and validate the weeding effectiveness of the device. The test setup consists of three main components: a test trolley, a weeding mechanism, and a soil trough. The weeding mechanism is securely mounted on the experimental trolley. The weeding cutter head, which is a part of the mechanism, is driven to move by controlling the electric actuator, allowing it to expand and contract accordingly. Please refer to Fig. 8 for a visual representation of the setup, which showcases the arrangement and positioning of the weeding mechanism (see Fig. 8a, b for test bed and test scene respectively), the experiment trolley, and the soil trough within the laboratory.

The test materials used in the experiment were corn seedlings at the 3 to 6 leaf stage and various accompanying weeds. Based on field research, the main types of weeds included wheat seedlings, Humulus, Dogwood, Matang, and Oxalis. These species are representative of common broadleaf and grassy weeds found in maize cultivation, ensuring that the experimental conditions closely mimic real-world scenarios. While the experiment was conducted in a controlled soil trough environment, variables such as soil type and moisture content were monitored and maintained at levels typical of cornfield conditions. To conduct the experiment, corn seeds and different weed seeds were collected from the ecological unmanned farm of Shandong University of Science and Technology. These seeds were initially planted in laboratory containers and allowed to germinate and develop into seedlings. Subsequently, the seedlings were transplanted to the soil troughs for the experiment.

The dimensions of the test soil trough were 20 m in length and 3 m in width. Each test run covered a distance of 10 m. The pre-weeding preparation area spanned 2 m, followed by a 6-meter-long corn planting area, and finally, a 2-meter-long post-weeding parking area. The maize planting rows were spaced 50 centimeters apart, with a plant spacing of 30 centimeters. The soil in the test soil trough had a water content of 13.4% in the 0–10-centimeter depth range. Additionally, the soil tightness was determined to be 87 kPa. These parameters were considered during the experiment to ensure proper testing conditions and accurate evaluation of the weeding device's performance. The movement speed of the weeding cutter head is the longitudinal velocity of the whole weeding system. Since it is propelled by a linear actuator, its speed is contingent upon the output velocity of the linear actuator. Experimental results have indicated that the weeding is most effective at a motion speed of 80 mm/s. Weeds are identified and located through a machine vision system. During operation, a camera captures images of the field which are then processed by a deep learning model to detect and ascertain the positions of weeds. The deep learning model is deployed on an embedded development board situated on the vehicle. As this component is not the focus of the present study, it is not elaborated upon in the text.

Test factors and indicators

In the previous theoretical analysis, the penetration of the weeding device into the soil and the movement speed of the weeding cutter head were identified as important factors affecting the weeding effectiveness of the spiral tendon weeding device. Additionally, it was determined that changes in electric actuator thrust significantly impacted weeding success rate.

To evaluate the operational effectiveness of the weeding device, three main working parameters were selected as the test factors: depth of entry, movement speed, and push rod thrust. The weeding rate and seedling injury rate were chosen as evaluation indexes[40,41].

The calculation formulas for the evaluation indexes are as follows:

$$\alpha = \frac{W_b - W_a}{W_b} \times 100\% \tag{12}$$

$$\beta = \frac{M_b}{M_a} \times 100\% \tag{13}$$

α is the weed control rate, %; W_b is the total weed count; W_a is the number of weeds remaining after mowing; β is the rate of seedling injury, %; M_b is the number of injured seedling plants after weeding; M_a is the total number of seedlings.

These evaluation indexes provide quantitative measures to assess the performance of the weeding device. The weed control rate indicates the effectiveness of weed removal, while the rate of seedling injury reflects the extent of damage inflicted on the desirable crop during the weeding process.

Experimental design

To investigate the influence of each working parameter (penetration of the weeding device into the soil, movement speed, and pusher thrust) on the weed removal rate and seedling wounding rate, a single-factor test was initially

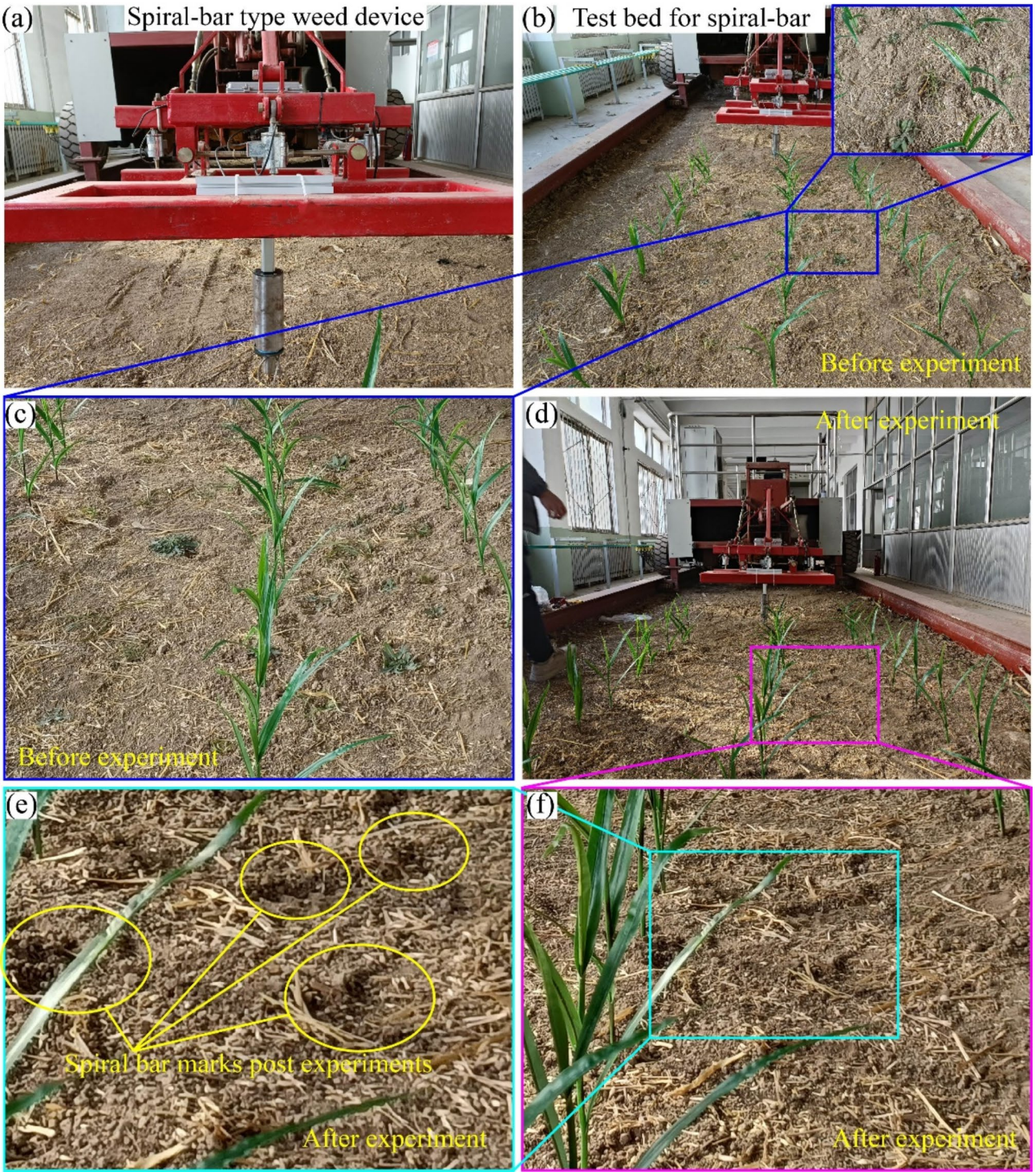

Fig. 8. (**a**) Spiral-bar type weed device. (**b**) Test scene of spiral-bar type weed device.

conducted using a homemade test stand. This preparatory test aimed to identify the impact of each parameter and determine their reasonable ranges of variation. The results of this single-factor test were then utilized to determine the factor levels for the subsequent orthogonal test. After determining the factor levels, a three-factor three-level orthogonal test was carried out. Table 1 provides a representation of these factor levels. This test aims to determine the degree of influence of the main factors on the experimental indicators and identify the optimal combination of factor parameters that leads to the optimal values of the evaluation indicators. By conducting the orthogonal test, the researchers aimed to assess the influence of each influencing factor on the experimental indicators. The ultimate goal was to identify the optimal combination of factor parameters that would maximize

Level (of achievement etc.)	Experimental factors		
	Depth of entry (mm)	Movement speed (mm/s)	Actuator thrust (*N*)
1	50	80	120
2	60	100	150
3	70	120	180

Table 1. Experimental factors and levels.

the evaluation indicators, thereby achieving the desired level of weed removal rate and minimizing seedling wounding rate.

Results

Analysis of the results of the one-way test

Depth of entry

Based on the provided information and Fig. 9a, we can make the following observations regarding the relationship between the penetration of the weeding device into the soil and the performance evaluation indexes:

① **Weed control rate**: As the depth of soil penetration increases, the weeding head initially rises sharply before gradually stabilizing. This phenomenon is attributed to deeper soil penetration enhanced ability to uproot deep-rooted weeds, resulting in a notable increase in the weed control rate. When the depth of soil penetration ranges from 40 to 60 mm, the weed control rate shows a faster increase, ranging from 73.7 to 89.0% as shown in Fig. 9a. However, when the depth of soil penetration ranges from 60 to 80 mm, the weed control rate increases less and tends to stabilize.

② **Seedling injury rate**: The rate of seedling injury increases with an increase in soil penetration depth. This is because the closer the spiral bar is to the seedling roots at the deepest soil penetration position, the greater the likelihood of causing damage to the seedling roots. The rate of seedling injury ranges from 2.1 to 4.1% as the soil penetration depth increases.

To achieve a better inter-plant weeding effect while considering the issue of seedling injury rate, it is suggested that a more appropriate depth of entry would be in the range of 50–70 mm. Within this range, a relatively high weed control rate can be achieved, while minimizing the risk of seedling injury.

Speed of movement

Based on the information provided and Fig. 9b, we can make the following observations regarding the relationship between the movement speed of the weeding cutter head and the weed removal rate:

① **Weed removal rate**: As the movement speed of the weeding cutter head increases, the weed removal rate slowly decreases. However, even at the highest movement speed tested, the weed removal rate remains above 80%. This indicates that within the range of test parameters for the movement speed of the weeding cutter head, the influence of speed on the operational performance of the weeding mechanism is relatively small.

To balance both the weed removal rate and seedling injury rate, it is recommended to control the movement speed of the weeding cutter head within the range of 80–120 mm/s. This range allows for a satisfactory weed removal rate while minimizing potential negative effects on seedling injury.

Actuator thrust

Based on the provided information and Fig. 9c, the following can be observed regarding the relationship between the push rod thrust and the weeding rate:

① **Weeding rate**: As increase in push rod thrust lead to significant changes in the weeding rate, ranging from 73.4 to 94.7%. This indicates the crucial role of push rod thrust in achieving effective weed removal. As higher thrust values generally result in higher weeding rates.

② **Seedling wounding rate**: the rate of seedling wounding initially increases slowly and then rises sharply as the push rod thrust increases. Within the range of 90 N to 180 N, the rate of seedling wounding gradually increases from 2 to 3.2%. However, when the push rod thrust increases from 180 N to 210 N, the rate of seedling wounding jumps significantly from 3.2 to 4.2%. This suggests that higher push rod thrust can potentially cause more damage to seedlings.

Taking into considering both the weeding rate and the rate of seedling injury, it is recommended to select a push rod thrust between 120 N and 180 N as the preferred value. Within this range, a relatively high weeding rate can be achieved, while minimizing the potential risk of seedling injury. Although a slightly higher weeding rate can be obtained at 210 N, it also results in a significant increase in the rate of seedling injury, making the range of 120 N to 180 N more suitable.

Analysis of orthogonal test results

The orthogonal test program and results are presented in Table 2, for designing of the orthogonal experimental combinations authors have followed previous literature[41]. In the table, A, B, and C represent the test factors: penetration of the weeding device into the soil, movement speed, and actuator thrust, respectively. To visually illustrate the effects of different parameter combinations on each evaluation index, line graphs are provided in Fig. 10.

From Fig. 10, it is evident that the weed removal effect on wheat seedlings is the most favorable, consistently exceeding 89%, and showing less sensitivity to parameter changes. In contrast, the control of the other four weed

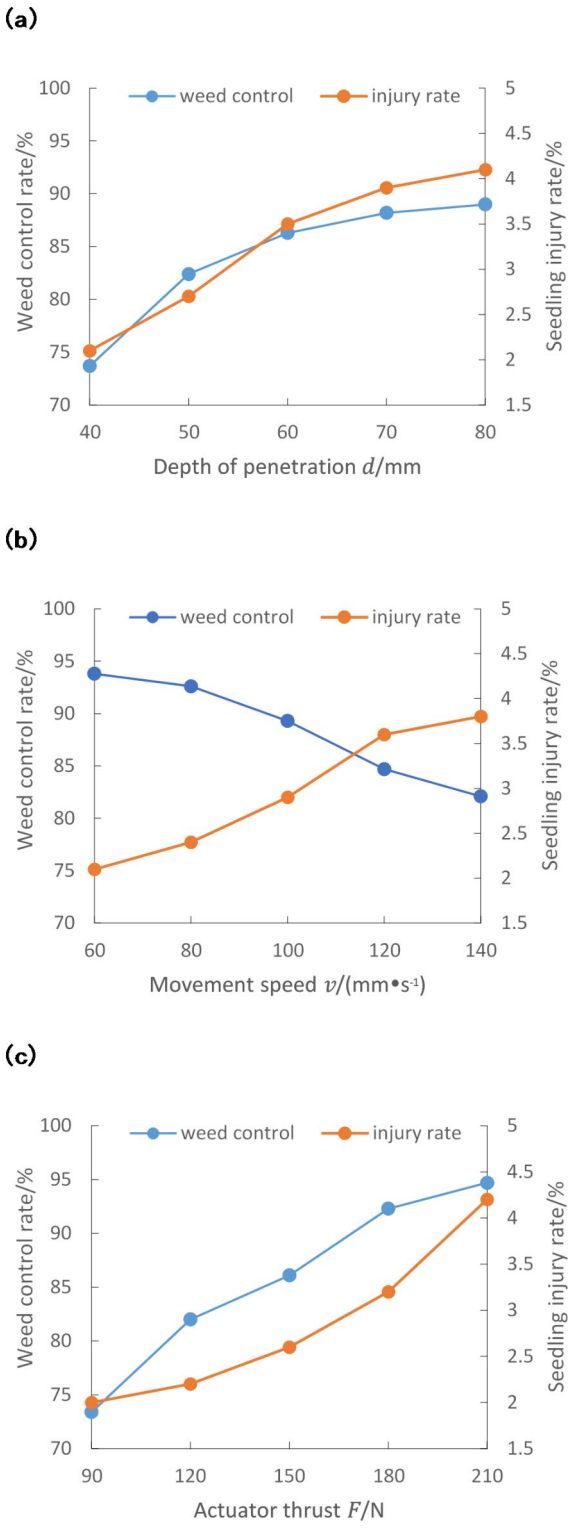

Fig. 9. Relationship between weed control rate and various factors. (**a**) Weed control rate and injury rate vs. depth of penetration. (**b**) Weed control rate and injury rate vs. movement speed. (**c**) Weed control rate and injury rate vs. actuator thrust.

types and the rate of injured seedlings fluctuates significantly with parameter variations but follow a relatively similar pattern.

To analyze these changes, we evaluated the average weed control rate and seedling injury rate using extreme differences and ANOVA, as shown in Tables 3 and 4. The analysis indicates that the primary and secondary factors affecting the weed control rate are C, A, and B, with the actuator thrust having the most significant effect,

Test number	Experimental factors			Test indicators	
	A	B	C	Weed removal rate (%)	Injury rate (%)
1	1	1	1	79.24	1.9
2	1	2	2	83.94	2.9
3	1	3	3	88.52	3.1
4	2	1	2	90.1	2.7
5	2	2	3	92.64	3.4
6	2	3	1	84.96	2.5
7	3	1	3	95.84	3
8	3	2	1	86.18	2.7
9	3	3	2	88.3	2.6

Table 2. Orthogonal test program and results.

followed by penetration of the weeding device into the soil, while the movement speed has a relatively smaller impact. Hence, the recommended program is A3 B1 C3, with a 70 mm penetration of the weeding device into the soil, a movement speed of 80 mm/s, and an actuator thrust of 180 N. Under this program, the weed control rate exceeds 95%, and the seedling injury rate is below 3% (see Tables 3 and 4).

Regarding the seedling injury rate, the analysis using extreme difference and ANOVA reveals that the primary and secondary factors influencing this rate are C, B, and A. The actuator thrust shows a significant effect, while the penetration of the weeding device into the soil and movement speed has a non-significant impact. Consequently, the preferred program is A1 B1 C1, with a 50 mm penetration of the weeding device into the soil, a movement speed of 80 mm/s, and an actuator thrust of 120 N. This program achieves a weed removal rate exceeding 95% and a seedling injury rate below 3%.

Based on the analysis, the optimal solution for inter-plant weeding is determined to be A3 B1 C3, with a 70 mm penetration of the weeding device into the soil for the weeding cutter head, a movement speed of 80 mm/s, and an actuator thrust output of 180 N. This program achieves a weed removal rate of over 95% and a seedling injury rate of 3% or lower. The selection of these specific parameters results from testing and optimization processes aimed at balancing effectiveness and minimizing harm to the crop. The values of 70-mm depth, 80 mm/s movement speed, and 180 N thrust were determined through a series of optimization tests that considered the balance between weed removal efficiency and minimizing crop damage. The 70-mm depth was selected based on the typical root depth of common weeds, ensuring effective uprooting without excessive soil disturbance. The movement speed of 80 mm/s was found to provide sufficient operational speed while maintaining control and precision. Finally, the 180 N thrust was chosen as it provided enough force to effectively penetrate the soil and remove weeds, while minimizing the risk of damaging the corn seedlings.

Conclusion

In conclusion, this paper presents a solution to the challenges associated with weed management in cornfields through the introduction of a spiral bar cornfield precision weeding device. Through meticulous mechanical design and theoretical analysis, the structural form and key parameters of the weeding components are determined, considering the physical characteristics of both corn seedlings and accompanying weeds.

This study proposes a spiral tendon-type precision weeding device tailored for corn fields, leveraging the theory of spiral motion. The device integrates an intelligent navigation platform, spiral tendon mechanism, and weeding cutter head to achieve precise and efficient weed removal while minimizing crop damage. Operating on the principle of spiral motion, the spiral bar-type weeding cutter head moves under the guidance of the intelligent navigation platform, facilitating controlled movements for effective weed removal.

Analyzing the force and motion characteristics of the spiral bar-type weeding cutter head is crucial for determining operational parameters. By scrutinizing force and motion laws, this analysis enables the derivation of the force required for effective soil penetration and the determination of the trajectory and speed of the cutter head's movement in the soil. Optimization of the contour shape of the inner cylinder track and its coordination mode with the roller follower plays a pivotal role in achieving the desired motion. Through comprehensive analysis, key parameters of the circulating track are derived, leading to an optimized design for efficient and precise weed removal in corn fields. Prototype trials and tests, encompassing bench tests and soil trench tests, were conducted to validate the operational performance of the weeding device. The objective was to confirm the effectiveness of the parameter optimization and structural design scheme for the device. Based on the results, optimal parameter combinations were derived: the depth of the weeding cutter head into the soil was 70-mm, the movement speed was 80 mm/s, and the output thrust of the electric actuator was 180 N. Employing these parameters, the weeding device demonstrated improved pulling efficiency, achieving an overall weed removal rate of over 95%, while maintaining a minimal seedling injury rate of 3%, satisfying the agronomic requirements for inter-plant weeding in maize fields. This technological innovation not only revolutionizes mechanical weeding device design but also significantly contributes to reducing reliance on chemical herbicides and advancing intelligent and ecological agriculture practices.

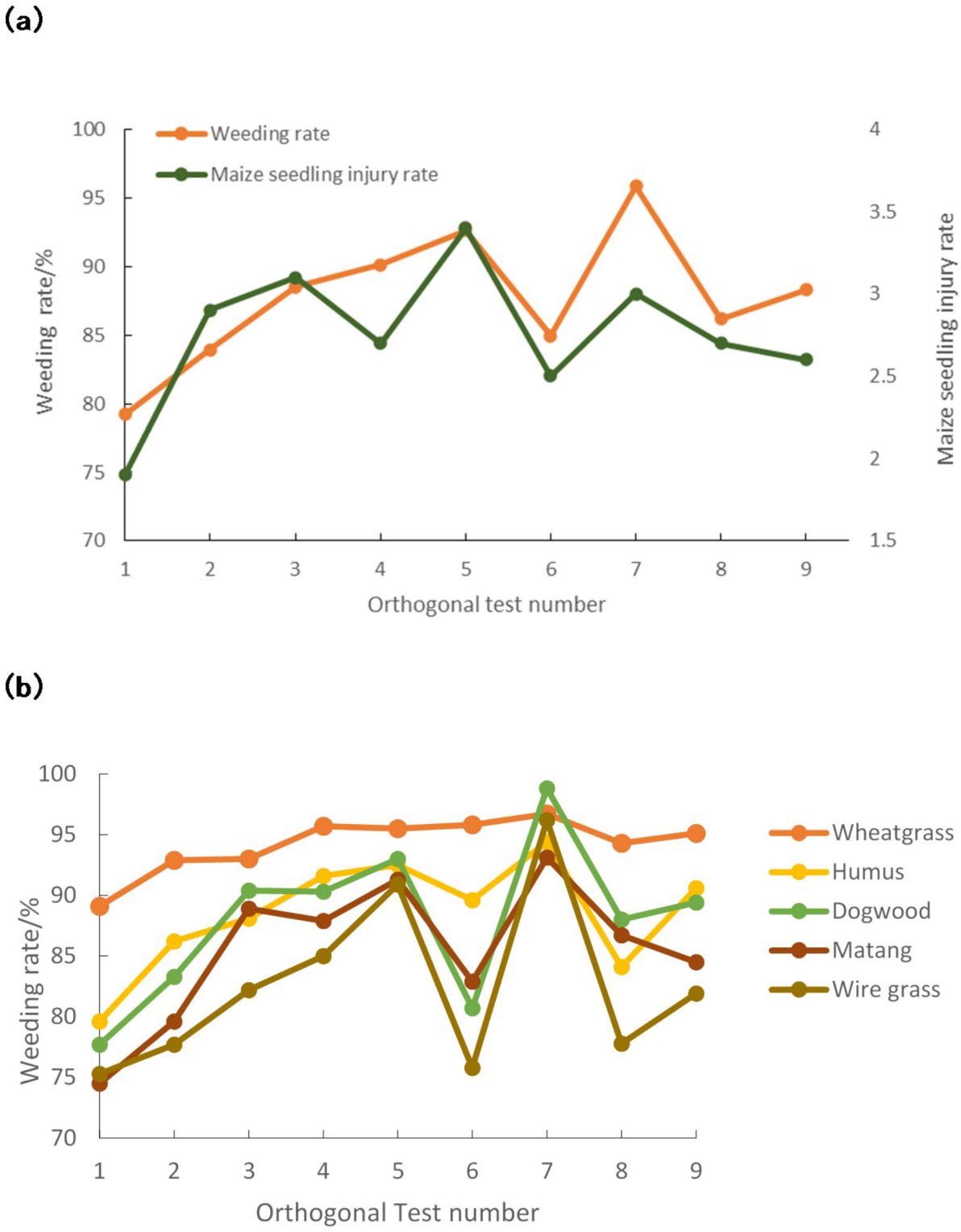

Fig. 10. Line graph of orthogonal test results. (**a**) Comparison of overall weeding rate and seedling damage rate. (**b**) Comparison of removal rates of various weeds.

Limitations and future improvements

Despite the promising results achieved with the spiral bar precision weeder, there are a few limitations that need to be addressed in future research. Firstly, the prototype and trials were conducted under controlled conditions that may not fully replicate the different environmental and soil conditions found in different maize fields. Factors such as soil moisture and the presence of different weed species could significantly affect the performance of the

	Experimental factors	A	B	C
Weed control	K1	83.9	88.39	83.46
	K2	89.23	87.59	87.45
	K3	90.11	87.26	92.33
	Polar deviation R	6.21	1.13	8.87
	Excellent level	A3	B1	C3
	Order of priority	C, A, B		
	Better program	A3 B1 C3		
Injury rate	K1	2.63	2.53	2.37
	K2	2.87	3	2.73
	K3	2.77	2.73	3.17
	Polar deviation R	0.23	0.47	0.8
	Excellent level	A1	B1	C1
	Order of priority	C, B, A		
	BETTER program	A1 B1 C1		

Table 3. Orthogonal test polar analysis.

Source of variance	A	B	C	inaccuracies
(a) ANOVA for weed control rate				
Square sum (e.g. equation of squares)	338.65	10.21	592.55	18.97
(Number of) degrees of freedom (physics)	2	2	2	2
Mean square and	169.32	5.1	296.27	9.48
F	17.85	0.54	31.24	
Significance	*	ns	**	
(b) Analysis of variance (ANOVA) for seedling injury rate				
Square sum (e.g. equation of squares)	0.082	0.329	0.962	0.069
(Number of) degrees of freedom (physics)	2	2	2	2
Mean square and	0.041	0.164	0.481	0.034
F	1.194	4.774	13.968	
Significance	ns	ns	*	

Table 4. Orthogonal test ANOVA. Note: Checking the F-distribution table shows that F0.10 (2,2) = 9.00, F0.05 (2,2) = 19.00, and F0.01 (2,2) = 99.00. Since F0.10 (2,2) < FA < F0.05 (2,2), it is considered as a significant impact and is denoted as *; FB < F0.10 (2,2), it is considered as a non-significant impact and is denoted as ns; and F0.10 (2,2) < FC < F0.05 (2,2), it is a highly significant effect, denoted as **.

device. Extensive field trials in different geographical locations and seasons are therefore required to validate the effectiveness and adaptability of the device.

Data availability

Data will be made available on request to corresponding author.

Received: 15 July 2024; Accepted: 14 October 2024
Published online: 15 November 2024

References

1. Wu, A., Elahi, E., Cao, F., Yusuf, M. & Abro M. I. sustainable grain production growth of farmland—A role of agricultural socialized services. *Heliyon.* **10** (2024).
2. Chen, M., Cheng, X., Jia, X., Zhang, L. & Li, Q. Optimization of operating parameter and structure for corn ear picking device by bionic breaking ear hand. *Trans. Chin. Soc. Agric. Eng.* **34**, 15–22 (2018).
3. Elahi, E., Khalid, Z., Tauni, M. Z., Zhang, H. & Lirong, X. Extreme weather events risk to crop-production and the adaptation of innovative management strategies to mitigate the risk: a retrospective survey of rural Punjab, Pakistan. *Technovation.* **117**, 102255 (2022).
4. Ahmad, F. et al. Effect of operational parameters of UAV sprayer on spray deposition pattern in target and off-target zones during outer field weed control application. *Comput. Electron. Agric.* **172**, 105350 (2020).
5. Zhong, Z., Peng, B. & Elahi, E. Spatial and temporal pattern evolution and influencing factors of energy–environmental efficiency: a case study of Yangtze River urban agglomeration in China. *Energy Environ.* **32**, 242–261 (2021).
6. Guan, H. et al. Improved gaussian mixture model to map the flooded crops of VV and VH polarization data. *Remote Sens. Environ.* **295**, 113714 (2023).

7. Haq, S. I. U., Tahir, M. N. & Lan, Y. Weed detection in wheat crops using image analysis and artificial intelligence (AI). *Appl. Sci.* **13**, 8840 (2023).
8. Haq, S. I. U., Raza, A., Lan, Y. & Wang, S. Identification of pest attack on corn crops using machine learning techniques. *Eng. Proc.* **56**, 183 (2023).
9. Li, J. G. et al. Review of mechanical weeding technique in field at home and abroad. *J. Agric. Mech. Res.* **10**, 57–65 (2006).
10. Ma, X., Qi, L., Liang, B., Tan, Z. & Zuo, Y. Present status and prospects of mechanical weeding equipment and technology in paddy field. *Trans. Chin. Soc. Agric. Eng.* **27**, 162–168 (2011).
11. Abbas, A., Elahi, E., Yousaf, K., Ahmad, R. & Iqbal, T. Quantification of mechanization index and its impact on crop productivity and socioeconomic factors. *Int. Agric. Eng. J.* **26**, 49–54 (2017).
12. Bueno, M. R., Cunha, J. P. R., Naves, M. G. & Tavares, R. M. Spray deposition and weed control using a conventional boom sprayer and an auxiliary boom sprayer, with reduced spray volumes. *Planta Daninha.* **32**, 447–454 (2014).
13. Huang, X. et al. Design method and experiment of machinery for combined application of seed, fertilizer and herbicide. *Int. J. Agric. Biol. Eng.* **12**, 63–71 (2019).
14. Melander, B., Lattanzi, B. & Pannacci, E. Intelligent versus non-intelligent mechanical intra-row weed control in transplanted onion and cabbage. *Crop Prot.* **72**, 1–8 (2015).
15. Pannacci, E., Lattanzi, B. & Tei, F. Non-chemical weed management strategies in minor crops: a review. *Crop Prot.* **96**, 44–58 (2017).
16. Gai, J., Tang, L. & Steward, B. L. Automated crop plant detection based on the fusion of color and depth images for robotic weed control. *J. Field Robot.* **37**, 35–52 (2020).
17. Nørremark, M., Griepentrog, H. W., Nielsen, J. & Søgaard, H. T. The development and assessment of the accuracy of an autonomous GPS-based system for intra-row mechanical weed control in row crops. *Biosyst. Eng.* **101**, 396–410 (2008).
18. Pérez-Ruíz, M., Slaughter, D. C., Fathallah, F. A., Gliever, C. J. & Miller, B. J. Co-robotic intra-row weed control system. *Biosyst. Eng.* **126**, 45–55 (2014).
19. Han, B., Shen, J. & Li, Y. Design and experiment on 3ZCF-7700 multi-functional weeding-cultivating machine. *Trans. Chin. Soc. Agric. Eng.* **27**, 124–129 (2011).
20. Kamath, R., Balachandra, M. & Prabhu, S. Crop and weed discrimination using laws' texture masks. *Int. J. Agric. Biol. Eng.* **13**, 191–197 (2020).
21. Chandel, N. S., Chandel, A. K., Roul, A. K., Solanke, K. R. & Mehta, C. R. An integrated inter- and intra-row weeding system for row crops. *Crop Prot.* **145**, 105642 (2021).
22. Jia, H., Li, S., Wang, G. & Liu, H. Design and experiment of seedling avoidable weeding control device for intertillage maize (Zea mays L). *Trans. Chin. Soc. Agric. Eng.* **34**, 15–22 (2018).
23. Huang, J. et al. Assimilation of remote sensing into crop growth models: current status and perspectives. *Agric. For. Meteorol.* **276–277**, 107609 (2019).
24. Shahbazi, N. et al. Assessing the capability and potential of LiDAR for weed detection. *Sensors.* **21**, 2328 (2021).
25. Melander, B. Optimization of the adjustment of a vertical axis rotary brush weeder for intra-row weed control in row crops. *J. Agric. Eng. Res.* **68**, 39–50 (1997).
26. Martelloni, L., Fontanelli, M., Frasconi, C., Raffaelli, M. & Peruzzi, A. Cross-flaming application for intra-row weed control in maize. *Appl. Eng. Agric.* **32**, 569–578 (2016).
27. Tang, D. et al. On the nonlinear time-varying mixed lubrication for coupled spiral microgroove water-lubricated bearings with mass conservation cavitation. *Tribol. Int.* **193**, 109381 (2024).
28. Duerinckx, K., Mouazen, A. M., Anthonis, J. & Ramon, H. Effects of spring-tine settings and operational conditions on the mechanical performance of a weed harrow tine. *Biosyst. Eng.* **91**, 21–34 (2005).
29. O'Dogherty, M. J., Godwin, R. J., Dedousis, A. P., Brighton, J. L. & Tillett, N. D. A mathematical model of the kinematics of a rotating disc for inter- and intra-row hoeing. *Biosyst Eng.* **96**, 169–179 (2007).
30. Xiong, Y., Ge, Y., Liang, Y. & Blackmore, S. Development of a prototype robot and fast path-planning algorithm for static laser weeding. *Comput. Electron. Agric.* **142**, 494–503 (2017).
31. Merfield, C. N. Robotic weeding's false dawn? Ten requirements for fully autonomous mechanical weed management. *Weed Res.* **56**, 340–344 (2016).
32. Ye, S. et al. Design and testing of an elastic comb reciprocating a soybean plant-to-plant seedling avoidance and weeding device. *Agriculture.* **13**, 2157 (2023).
33. Mao, W., Zhang, Y., Wang, H., Zhao, B. & Zhang, X. Advance techniques and equipments for real-time weed detection. *Nongye Jixie Xuebao.* **44**, 190–195 (2013).
34. Ziwen, C. et al. Study review and analysis of high performance intra-row weeding robot. *Trans. Chin. Soc. Agric. Eng.* **31**, 1–8 (2015).
35. Hu, L. et al. Development and experiment of intra-row mechanical weeding device based on trochoid motion of claw tooth. *Trans. Chin. Soc. Agric. Eng.* **28**, 10–16 (2012).
36. Zhou, F., Wang, W., Li, X. & Tang, Z. Design and experiment of cam rocker swing intra-row weeding device for maize. *Nongye Jixie Xuebao.* **49** (2018).
37. Huang, H. et al. The improved winter wheat yield estimation by assimilating GLASS LAI into a crop growth model with the proposed bayesian posterior-based ensemble Kalman filter. *IEEE Trans. Geosci. Remote Sens.* **61**, 1–18 (2023).
38. Potts, D. M., Zdravković, L., Addenbrooke, T. I., Higgins, K. G. & Kovačević, N. *Finite Element Analysis in Geotechnical Engineering: Application*vol. 2 (Thomas Telford London, 2001).
39. Al-Awad, M. N. J. Simple correlation to evaluate Mohr–Coulomb failure criterion using uniaxial compressive strength. *J. King Saud Univ. Eng. Sci.* **14**, 137–144 (2002).
40. Jinqing, L. et al. Design and experiment of driving-type crushing-weeding multi-functional potato cultivator. *Trans. Chin. Soc. Agric. Eng.* **35**, 1–8 (2019).
41. Wang, J. et al. Design and experiment of curved-tooth oblique type inter-row weeding device for paddy field. *Nongye Jixie Xuebao.* **52** (2021).

Acknowledgements

The authors extend their appreciation to the Deanship of Scientific Research at King Khalid University for funding this work through large Groups Project under grant number RGP.2/591/45.

Author contributions

Wenze Hu; Conceptualization, methodology, software, validation, formal analysis, investigation, resources, data curation, writing—original draft preparation.Syed Ijaz Ul Haq; Conceptualization, methodology, software, validation, formal analysis, investigation, writing—review and editing.Yubin Lan; Supervision, Proof reading, Project administration.Zhihuan Zhao; Writing—review and editing.Shadab Ahmad; Mechanical & formal analysis, Writing—review and editing.Areej Al Bahir; Writing—review and editing.Junke Zhu; Resources, data curation,

& investigation.Atiku Bran; Formal analysis, Writing—review and editing.

Funding
The current work was assisted financially to the Dean of Science and Research at King Khalid University via the Large Group Project under grant number RGP.2/591/45.

Declarations

Competing interests
The authors declare no competing interests.

Additional information
Correspondence and requests for materials should be addressed to J.Z. or A.B.

Reprints and permissions information is available at www.nature.com/reprints.

Publisher's note Springer Nature remains neutral with regard to jurisdictional claims in published maps and institutional affiliations.